

Effect of stenting on the near-infrared spectroscopy-derived lipid core burden index of carotid artery plaque



Cyril Štěchovský*, MD; Petr Hájek, MD, PhD; Martin Horváth, MD; Josef Veselka, MD, PhD

Department of Cardiology, Second Faculty of Medicine, Charles University, University Hospital Motol, Prague, Czech Republic

This paper also includes supplementary data published online at: <https://eurointervention.pconline.com/doi/10.4244/EIJ-D-17-01054>

KEYWORDS

- carotid and super-aortic disease
- carotid stenting
- imaging modalities
- other imaging modalities

Abstract

Aims: Catheter-based intravascular near-infrared spectroscopy (NIRS) detects a lipid signal from atherosclerotic plaque. The aim of this study was to describe the effect of carotid artery stenting (CAS) on the lipid signal in a carotid stenosis.

Methods and results: We performed NIRS combined with intravascular ultrasound (IVUS) during 120 CAS procedures. Minimal luminal area (MLA) and plaque burden (PB) at the site of MLA were measured with IVUS and lipid core burden index (LCBI), maximal LCBI in a 4 mm segment of the artery (LCBI_{max}) and LCBI in a 4 mm segment at the site of MLA (LCBI_{mla}) with NIRS-derived chemograms. NIRS-IVUS imaging was performed at baseline, after stent implantation and after balloon post-dilatation. The most common lesion type was the fibrocalcific plaque (76%). Lipid-rich plaque (LCBI_{max} ≥400) was present in 33% of carotid stenoses and in 20% at the site of MLA. Median MLA increased significantly from baseline to stent implantation (3.63 mm² to 5.56 mm², p<0.001) and to post-dilatation (5.56 mm² to 12.03 mm², p<0.001). Median LCBI, LCBI_{max} and LCBI_{mla} significantly decreased from baseline to stent implantation: LCBI (60 to 8, p<0.001), LCBI_{max} (294 to 60, p<0.001) and LCBI_{mla} (124 to 0, p<0.001). Post-dilatation of the stent had no further significant effect on median LCBI (8 to 5, p=0.890), LCBI_{max} (60 to 50, p=0.690) and LCBI_{mla} (0 to 0, p=0.438).

Conclusions: Carotid artery stenting significantly reduced the NIRS-derived lipid core burden index at the stented segment.

*Corresponding author: Department of Cardiology, Motol University Hospital, V Uvalu 84, 150 06 Prague, Czech Republic.
E-mail: stechovsky@gmail.com

Abbreviations

CAS	carotid artery stenting
CCA	common carotid artery
CSA	cross-sectional area
EEM	external elastic membrane
EEMCSA_{lcbimax}	external elastic membrane cross-sectional area at the site of maximal lipid core burden index
EEMCSA_{mla}	external elastic membrane cross-sectional area at the site of minimal luminal area
EEMCSA_{ref}	external elastic membrane cross-sectional area at the site of reference section
ICA	internal carotid artery
IVUS	intravascular ultrasound
LCBI	lipid core burden index
LCBI_{max}	maximal lipid core burden index in any 4 mm segment of the artery
LCBI_{mla}	lipid core burden index in the 4 mm segment at the site of minimal luminal area
LCP	lipid core plaque
LRP	lipid-rich plaque
LumenCSA	lumen cross-sectional area
MLA	minimal luminal area
NIRS	near-infrared spectroscopy
PB	plaque burden
PB_{lcbimax}	plaque burden at the site of maximal lipid core burden index
PB_{mla}	plaque burden at the site of minimal luminal area
RI	remodelling index
ROI	region of interest
TIA	transient ischaemic attack

Introduction

Advances in invasive and non-invasive vascular imaging have led to better understanding of the pathophysiology of atherosclerosis. However, most of the *in vivo* studies were performed on coronary arteries. Catheter-based intravascular near-infrared spectroscopy (NIRS) is a relatively novel imaging method to detect a lipid signal from an atherosclerotic plaque^{1,2}. The accuracy of NIRS to detect lipid core-containing atherosclerotic plaques has been validated in coronary autopsy specimens¹ and *in vivo*². NIRS has been utilised to assess coronary atherosclerosis and the effect of various interventions on the lipid signal in coronary plaques³⁻⁵. Studies with NIRS have demonstrated that the presence of lipid-rich coronary plaques in patients undergoing percutaneous coronary intervention (PCI) is related to the incidence of cardiovascular events during long-term follow-up^{6,7}, the risk of periprocedural myocardial infarction during PCI⁸⁻¹⁰, and presentation with stable angina versus acute coronary syndrome^{11,12}. They further described the coronary artery response to PCI as redistribution and reduction of the lipid core in the stented segment¹³⁻¹⁵. A similar response to stent implantation (i.e., reduction of the lipid signal) could be expected in other vascular territories. We have already reported

the safety and feasibility of the NIRS-IVUS imaging of carotid arteries *in vivo* and the distribution of LCBI in carotid stenosis¹⁶ and improved characterisation of the composition of carotid stenosis with multimodality imaging including NIRS¹⁷.

The aim of this study was to describe the effect of carotid artery stenting (CAS) on the lipid signal in a carotid stenosis. The response of the lipid signal was assessed with intravascular NIRS-derived lipid core burden index (LCBI) in a segment of common and internal carotid artery before and after stent implantation.

Methods

DESIGN

In Motol University Hospital, Prague, Czech Republic, we prospectively enrolled patients undergoing CAS who met the eligibility criteria into the registry. The study protocol was approved by the Motol University Hospital Ethics Committee. All patients provided written informed consent for their participation. Imaging with NIRS-IVUS was performed prior to stent implantation (baseline), after stent implantation and after balloon post-dilatation.

STUDY POPULATION

Patients were referred to CAS by a neurologist, cardiologist or vascular surgeon based on Doppler ultrasound and/or CT angiography imaging. Doppler ultrasound was available in 104 (87%) and CT angiography in 51 (43%) carotid stenoses. Stenoses were quantified angiographically according to the North American Symptomatic Carotid Endarterectomy Trial Collaborators criteria¹⁸. Inclusion criteria were symptomatic ($\geq 50\%$) or asymptomatic ($\geq 70\%$) stenosis of the internal carotid artery (ICA) in a patient who was considered eligible for CAS with a protection device. Eligibility criteria were in accordance with the ESC Guidelines on the diagnosis and treatment of peripheral artery diseases¹⁹. Exclusion criteria were prior ipsilateral CAS, advanced heart failure, renal insufficiency with an eGFR ≤ 30 mL/min/1.73 m², active bleeding, history of intracranial bleeding, imaging evidence of intraluminal thrombus, lesions with angiographic string sign or near occlusion and where the carotid anatomy was deemed inappropriate for NIRS-IVUS imaging (kinking, severe tortuosity). Carotid stenosis was considered symptomatic if the patient suffered from stroke, transient ischaemic attack or amaurosis fugax ipsilateral to the stenosis in the previous six months.

CAROTID STENTING

The CAS procedures were all performed by an experienced operator^{20,21}. Procedures were performed using a 7 or 8 Fr guiding catheter or a long 6 Fr sheath. The antithrombotic regimen included administration of 100 mg of aspirin and 300 mg of clopidogrel before CAS; a bolus of heparin (70 IU/kg) was administered at the beginning of CAS. Types and manufacturers of the embolic protection devices and stents are listed in **Supplementary Table 1**. Use of an embolic protection device was mandatory prior to NIRS-IVUS imaging. Stents were post-dilatated in 98% of the procedures with a 4-5 mm angioplasty balloon up to 8 atmospheres.

NEAR-INFRARED SPECTROSCOPY AND INTRAVASCULAR ULTRASOUND IMAGING TECHNIQUE

NIRS and IVUS were performed utilising a single 3.2 Fr rapid-exchange catheter TVC Insight™ Imaging System™ (Infraredx, Burlington, MA, USA). The system utilises absorbance and back-scattering of the near-infrared wavelength to determine chemical composition¹. The result of NIRS examination is presented as a chemogram – a two-dimensional map with the x-axis indicating the position of the measurement on the long axis of the vessel and the y-axis circumferential position of the measurement on the cross-section through the vessel – where every picture element (pixel) represents one spectroscopic measurement. Every measurement is binary coded as yellow (positive) or red (negative). The LCBI is a summary measure of the lipid signal along the interrogated segment of the vessel on a scale of 0 to 1,000. The LCBI is calculated as a fraction of yellow pixels in the chemogram multiplied by a factor of 1,000¹. The NIRS probe at the distal tip of the catheter acquires 40 spectroscopic measurements per second during automated pullback through the catheter at a speed of 0.5 mm/s and 16 rotations per second¹. IVUS images are acquired via a 40 MHz transducer rotating at the same speed as the NIRS probe.

Three NIRS-IVUS measurements were performed during one CAS procedure (Figure 1). Ten lesions (8%) required predilatation with a 2.0 mm balloon to facilitate passage of the catheter. The first pullback was performed prior to stent implantation (i.e., at baseline). The NIRS-IVUS catheter was advanced over a 0.014" guidewire into the ICA distal to the stenosis, and pullback was performed through the stenosis into the common carotid artery (CCA). The region of interest (ROI) was defined from IVUS as a 40 mm segment of the ICA and CCA corresponding to the landing zone of the stent. The second pullback was performed after stent implantation from the distal to the proximal edge of the stent. The third pullback was performed after balloon post-dilatation of the stent.

INTRAVASCULAR ULTRASOUND ANALYSIS AND DEFINITIONS

Off-line quantitative greyscale IVUS analysis was performed using the QIvus™ software (Medis, Leiden, the Netherlands). The definitions of the IVUS measurements are reported in the expert consensus document²² (Supplementary Appendix 1). IVUS was used to assess minimal luminal area (MLA), plaque burden (PB) and calcifications. Plaques at the site of MLA were defined as fibrocalcific if any calcifications were present and fibrous if there were no calcifications.

NEAR-INFRARED SPECTROSCOPY ANALYSIS AND DEFINITIONS

Off-line quantitative and qualitative analysis of NIRS-derived chemograms in the ROI was performed using the QIvus software (Medis). Chemograms were available in all 120 cases at baseline, in 114 cases (94%) after stent implantation and in 114 cases (94%) after post-dilatation. At least two chemograms were available in all

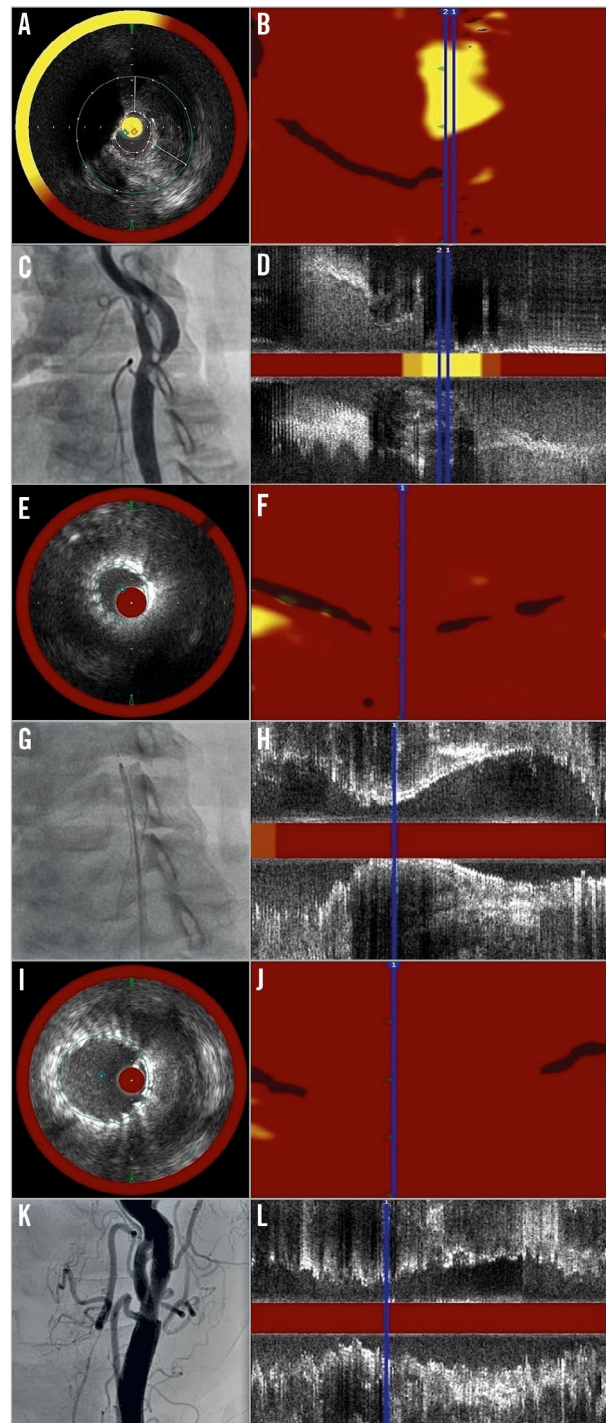


Figure 1. A panel of pictures demonstrating the imaging process in the study. A) – D) Imaging at baseline. E) – H) Imaging after stenting. I) – L) Imaging after balloon post-dilatation. A), E) & I) Cross-section NIRS-IVUS frames at the site of minimal lumen area. B), F) & J) Chemograms. C), G) & K) Angiograms of carotid bifurcation. D), H) & L) Corresponding longitudinal NIRS-IVUS images.

patients. The following parameters were used to quantify the lipid signal from the ROI: LCBI, maximal LCBI in any 4 mm segment of the artery (LCBI_{max}) and LCBI in the 4 mm segment at the site of minimal luminal area (LCBI_{mla}), defined as the segment 2 mm

proximal to 2 mm distal from the site of MLA. A lipid-rich plaque (LRP) was defined as a minimum 4 mm segment on the chemogram with LCBI_{max} ≥ 400 as previously described^{7,8,19}. Lipid core shift was defined as a new lipid signal (yellow spot) in a minimum 2 mm segment of a chemogram (yellow 2 mm block chemogram) which was free of the lipid signal (red 2 mm block chemogram) on the previous chemogram.

STATISTICAL ANALYSIS

Statistical analyses were performed using GraphPad Prism 6 software (GraphPad Software, La Jolla, CA, USA). Normally distributed continuous variables are presented as mean \pm standard deviation (SD) and compared with the Student's t-test. Non-parametric continuous variables are presented as median and interquartile range (IQR) and compared with a Wilcoxon matched-pair signed-rank test for paired samples or a Mann-Whitney U test for independent samples. Categorical variables are presented as frequency (%) and compared with Pearson's χ^2 test. A linear association between continuous variables is expressed with correlation plots and Pearson's correlation coefficient (r). A two-sided p-value of 0.05 or less was considered to indicate statistical significance.

Results

BASELINE AND PROCEDURAL CHARACTERISTICS

Between April 2013 and June 2017, 159 patients underwent 173 CAS procedures at the study institution. Periprocedural NIRS-IVUS imaging was performed in 120 CAS procedures in 112 patients (**Table 1**). The mean patient age was 67 \pm 8 years and two thirds were male. There was a high prevalence of hypertension (87%), coronary artery disease (50%), smoking (41%) and diabetes (37%). Two thirds of patients were considered to be high-risk for surgery. The procedural characteristics are listed in **Table 2**. Technical success of CAS (residual stenosis less than 30%) was achieved in all patients. All 120 (100%) patients underwent a 30-day follow-up. Two (1.7%) periprocedural TIAs occurred. During the 30-day follow-up two (1.7%) patients suffered from an ipsilateral stroke and there were no fatal events.

NEAR-INFRARED SPECTROSCOPY AND INTRAVASCULAR ULTRASOUND ASSESSMENT OF CAROTID STENOSIS

NIRS-IVUS provided several detailed insights into carotid stenosis (**Table 3**). Fibrocalcific and lipid-rich plaques at the site of MLA were present in 76% and 20% of cases, respectively. LRP in the whole ROI was identified in 33% of cases. Although baseline median LCBI_{max} was significantly higher than median LCBI_{mla} (294 [157-449] vs. 124 [0-338], $p < 0.001$), plaque burden (PB) at the site of MLA was significantly larger than PB at the site of LCBI_{max} (PB_{mla} 88.5 \pm 5.2% vs. PB_{lcbimax} 63.7 \pm 20.0%, $p < 0.001$). We constructed correlation plots for IVUS-derived measurements and LCBI (**Figure 2**). There was only a weak linear correlation between MLA and LCBI_{mla} ($r = -0.183$, $p = 0.045$) and no correlation between PB and LCBI_{mla} ($r = 0.104$, $p = 0.433$). Median LCBI,

Table 1. Patient characteristics.

	n (%)
Male	75 (67)
Age (years)	67.4 \pm 8.1
Body mass index (kg/m ²)	28.0 \pm 4.0
Symptomatic stenosis	17 (14)
Coronary artery disease	60 (50)
Diabetes	44 (37)
Arterial hypertension	104 (87)
Smoking	49 (41)
High-risk patient*	78 (65)
Medication	
Statin	92 (77)
Aspirin	101 (84)
Beta-blocker	66 (55)
RAAS inhibitor	89 (74)
Serum laboratory tests	
Total cholesterol (mmol/l)	4.32 \pm 0.93
Low-density lipoprotein cholesterol (mmol/l)	2.44 \pm 0.83
Creatinine (μ mol/l)	84.8 \pm 24.8
Estimated glomerular filtration rate (ml/s/1.73 m ²)	91 \pm 25
High-sensitivity C-reactive protein (mg/l)	4.8 \pm 8.9

* One of the following: left ventricular ejection fraction $\leq 40\%$, chronic bronchopulmonary disease, prior myocardial infarction, coronary artery bypass grafts or age ≥ 75 years.

LCBI_{max} and LCBI_{mla} did not differ significantly between sexes, symptomatic or asymptomatic stenoses, presence or absence of coronary artery disease and statin treatment status (**Supplementary Table 2**).

Table 2. Procedural characteristics.

Left carotid as a target vessel	67 (56%)	
Diameter stenosis at angiography, %	84 \pm 9	
Residual stenosis at angiography after CAS, %	8 \pm 8	
Use of protection device	100 (100%)	
Proximal occlusion device*	16 (13%)	
Distal filter device*	113 (94%)	
Direct stenting	110 (92%)	
Post-dilatation	117 (98%)	
Stent type	Number of implanted stents	129 (100%)
	Open-cell stent	33 (26%)
	Hybrid stent	13 (10%)
	Closed-cell stent	83 (64%)
Stent length, mm	37 \pm 5	
Fluoroscopy time, minutes	8.0 \pm 3.6	
Procedural time, minutes	27.4 \pm 9.2	

* Both devices could be used during one procedure. CAS: carotid artery stenting

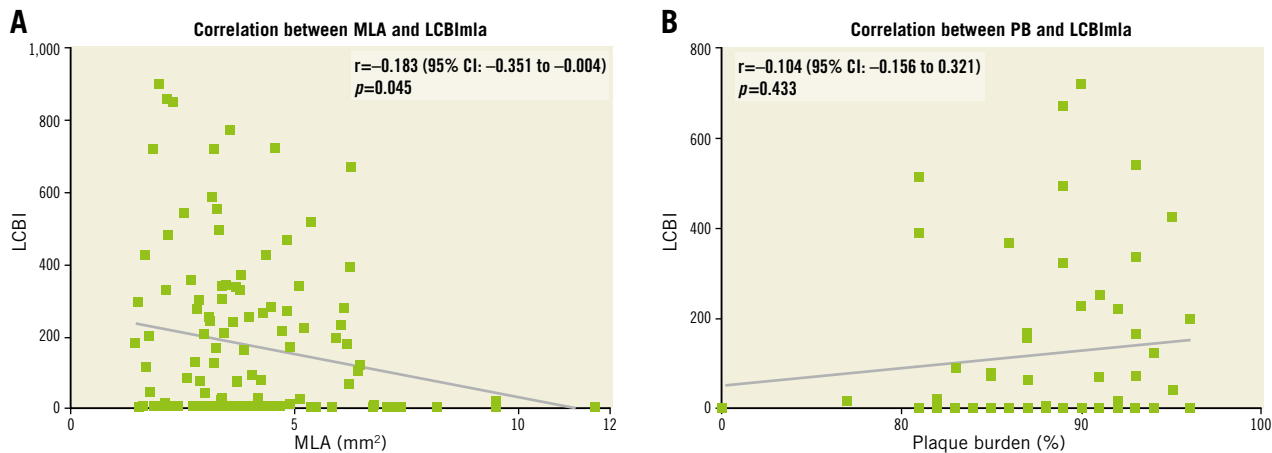


Figure 2. Correlation plots with Pearson's correlation coefficient (r). A) Correlation between LCBImla and minimal luminal area. B) Correlation between LCBImla and plaque burden.

CHANGE IN NEAR-INFRARED SPECTROSCOPY-DERIVED LIPID CORE SIZE DURING CAROTID STENTING

Median MLA increased significantly from baseline to stent implantation (3.63 mm^2 to 5.56 mm^2 , $p < 0.001$) and from stent implantation to post-dilatation (5.56 mm^2 to 12.03 mm^2 , $p < 0.001$) (Figure 3A). Median (IQR) LCBI (Figure 3B), LCBI_{max} (Figure 3C) and LCBI_{mla} (Figure 3D) decreased significantly from baseline to stent implantation: LCBI (60 [26-116] to 8 [1-33], $p < 0.001$), LCBI_{max} (294 [157-449] to 60 [9-217], $p < 0.001$) and LCBI_{mla} (124 [0-338] to 0 [0-2], $p < 0.001$). Post-dilatation of the stent had no further significant effect on median LCBI (8 [1-33] to

5 [0-38], $p = 0.890$), LCBI_{max} (60 [9-217] to 50 [0-224], $p = 0.690$) and LCBI_{mla} (0 [0-2] to 0 [0-0], $p = 0.438$). No significant difference in LCBI was observed after stenting with an open-cell stent versus a closed- or hybrid-cell stent (Supplementary Table 3). Lipid core shift was observed in 16 (13%) cases after stent implantation and in 27 (23%) cases after post-dilatation.

Discussion

The present study was the first prospective study to use serial NIRS-IVUS imaging in patients undergoing CAS to investigate lumen, plaque and lipid core changes caused by stent implantation and balloon post-dilatation. The major findings are summarised as follows. Plaques from severe carotid stenosis were mostly fibro-calcific but one third also contained lipid-rich regions. These LRP were at sites with a high plaque burden. Implantation of a self-expanding carotid stent, although resulting only in modest luminal expansion, led to a significant decrease in the LCBI. On the other hand, post-dilatation of the stent with an angioplasty balloon caused much greater lumen expansion but did not result in any further significant change in LCBI and was associated with lipid core shift in 23% of cases.

Recently published studies reported favourable long-term outcomes of both endarterectomy and stenting of carotid stenosis^{23,24}. Whereas endarterectomy restores the lumen diameter and removes the plaque, stenting restores the lumen by pushing the plaque outwards and, because it cannot be compressed, distending the media and external elastic membrane. The novel finding from our study is that CAS not only dilates the lumen but also significantly reduces the lipid signal. Whether this reduction also means long-term stabilisation after healing of the stent with neointima, hence the comparable long-term clinical effect of the two fundamentally different procedures – stenting and endarterectomy – requires further study. We assume that several mechanisms could have contributed to the observed reduction of the LCBI after stent implantation.

Table 3. NIRS-IVUS characteristics of the carotid stenosis.

NIRS-IVUS performed at	Baseline	120 (100%)
	After stent implantation	114 (95%)
	After post-dilatation	114 (95%)
Minimal luminal diameter, mm		1.94 ± 0.42
Reference luminal diameter, mm		4.34 ± 0.82
Minimal luminal area, mm^2		3.99 ± 1.77
Plaque burden at the site of MLA, %		88.5 ± 5.2
Plaque burden at the site of LCBI _{max} , %		63.7 ± 20.0
Lipid-rich plaque (LCBI _{max} ≥ 400)		40 (33%)
Arc of calcium at the site of MLA	0°	29 (24%)
	1-90°	43 (36%)
	91-180°	35 (29%)
	181-360°	13 (11%)
Type of plaque in the 4 mm segment with MLA	Fibrocalcific plaque	91 (76%)
	Lipid-rich plaque (LCBI _{mla} ≥ 400)	24 (20%)
	Non-calcified lipid-rich plaque (LCBI _{mla} ≥ 400)	4 (3%)
LCBI _{max} : maximal lipid core burden index in any 4 mm segment of the artery; LCBI _{mla} : lipid core burden index in the 4 mm segment at the site of minimal luminal area; MLA: minimal luminal area; NIRS-IVUS: near-infrared spectroscopy intravascular ultrasound		

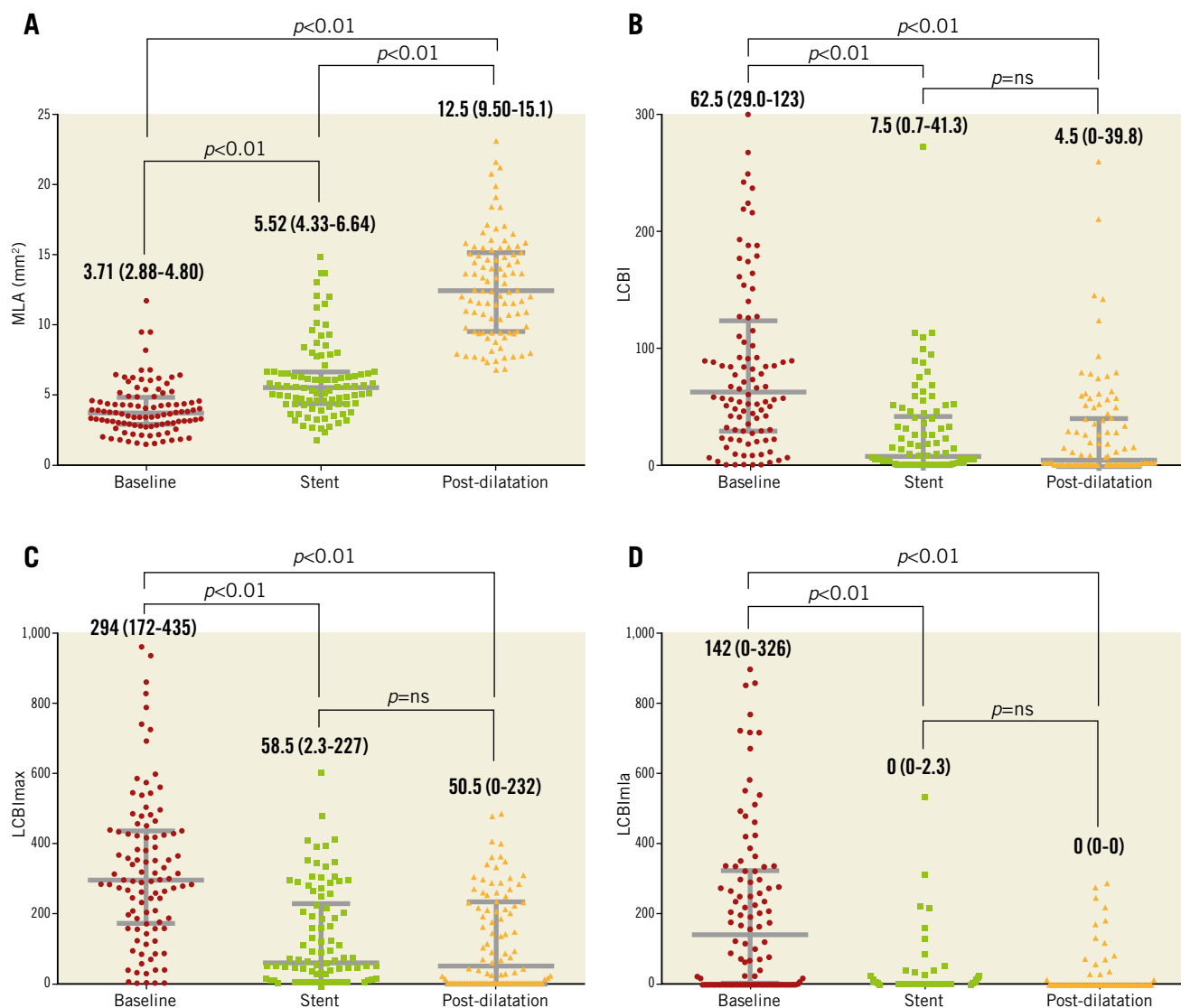


Figure 3. Scatter plots with median and IQR bars of A) minimal luminal area, B) lipid core burden index (LCBI), C) maximal lipid core burden index in any 4 mm segment of the artery (LCBI_{max}) and D) lipid core burden index in the 4 mm segment at the site of minimal luminal area (LCBI_{mla}) at baseline, after implantation of the stent and after post-dilatation of the stent.

The stent disrupts the fibrous cap and cuts into the soft lipid core, causing embolisation of the semi-liquid content. This might be the “culprit” in most ischaemic strokes that occur during or within hours to days after CAS, either by embolisation of the lipid core or by protrusion of the lipid-rich plaque through stent struts followed by thrombosis on the disrupted plaque and delayed embolisation. This mechanism was proposed for lipid-rich plaque-related myocardial infarction after PCI⁸⁻¹⁰ and was also observed with an optical coherence tomography (OCT) imaging during CAS^{25,26}. The limited size of our study and low incidence of adverse clinical events do not allow us to draw any conclusions regarding lipid core embolisation.

The stent causes compression and shift of the lipid core within the plaque. Lumen expansion increases the distance of the catheter from the lipid core, thus attenuating the lipid signal which

would not be actual lipid core reduction. Lipid core shift was observed in 23% of cases after post-dilatation as new yellow spots in segments that were without any lipid signal on the baseline chemogram.

The stent reflects near-infrared light obscuring the signal from the lipid core compressed under it. When the stent is not fully expanded, the struts are very dense and cover a significant proportion of the luminal area, creating a mirror to the near-infrared light beam. This would again lead to decreased LCBI, which would not be actual reduction of the lipid core. Post-dilatation decreases the density of the stent struts, which could make the lipid core compressed under the stent reappear on NIRS. Some cases of lipid core shift when there was major reduction of LCBI after stent implantation and some increase after post-dilatation could be explained by this mechanism.

Limitations

The present study is not without inherent limitations, mainly due to the *in vivo* setting. First, we did not routinely use any imaging method to detect silent microembolisation during CAS or new ischaemic lesions in the brain, which could be attributed to lipid core embolisation. Second, detection of lipid core with NIRS was not compared with another imaging method, as there is no gold standard for plaque composition *in vivo*. Nevertheless, in an appropriately sized lumen, there is no reason to expect NIRS signals to differ between the carotid and coronary arteries. In our study, the mean minimal luminal diameter of the ICA was 1.94 ± 0.42 mm, and the mean reference luminal diameter of the ICA was 4.34 ± 0.82 mm. The manufacturer of the TVC Imaging System reports a maximal imaging depth of 10 mm for IVUS and 3.5 mm for NIRS^{1,2}, assuming that the imaging depth should be sufficient for stenosis of the ICA.

Conclusions

Carotid artery stenting significantly reduced the NIRS-derived lipid core burden index at the stented segment. During CAS, a significant reduction of LCBI was observed after stent implantation, whereas post-dilatation of the stent had no further significant effect on LCBI.

Impact on daily practice

NIRS-IVUS assessment of the carotid stenosis in patients undergoing CAS provides additional morphological and compositional information that might prove useful in tailoring the treatment strategy. The best treatment option (specifically designed stents, aggressive antithrombotic and lipid-lowering therapy or endarterectomy) for lipid-rich carotid plaques needs to be determined in future trials.

Funding

This work was supported by the Ministry of Health, Czech Republic – conceptual development of research organisation, Motol University Hospital, Prague, Czech Republic. Grant number SVV-2013-266509 from the Charles University in Prague.

Conflict of interest statement

The authors have no conflicts of interest to declare.

References

- Gardner CM, Tan H, Hull EL, Lisauskas JB, Sum ST, Meese TM, Jiang C, Madden SP, Caplan JD, Burke AP, Virmani R, Goldstein J, Muller JE. Detection of lipid core coronary plaques in autopsy specimens with a novel catheter-based near-infrared spectroscopy system. *JACC Cardiovasc Imaging*. 2008;1:638-48.
- Waxman S, Dixon SR, L'Allier P, Moses JW, Petersen JL, Cutlip D, Tardif JC, Nesto RW, Muller JE, Hendricks MJ, Sum ST, Gardner CM, Goldstein JA, Stone GW, Krucoff MW. In vivo validation of a catheter-based near-infrared spectroscopy system for detection of lipid core coronary plaques: initial results of the SPECTACL study. *JACC Cardiovasc Imaging*. 2009;2:858-68.
- Roleder T, Kovacic JC, Ali Z, Sharma R, Cristea E, Moreno P, Sharma SK, Narula J, Kini AS. Combined NIRS and IVUS imaging detects vulnerable plaque using a single catheter system: a head-to-head comparison with OCT. *EuroIntervention*. 2014;10:303-11.
- Ten Haaf ME, Rijndertse M, Cheng JM, de Boer SP, Garcia-Garcia HM, van Geuns RM, Regar E, Lenzen MJ, Appelman Y, Boersma E. Sex differences in plaque characteristics by intravascular imaging in patients with coronary artery disease. *EuroIntervention*. 2017;13:320-8.
- Hildebrandt HA, Patsalis PC, Al-Rashid F, Neuhäuser M, Rassaf T, Heusch G, Kahlert P, Kleinbongard P. Quantification and characterisation of released plaque material during bioresorbable vascular scaffold implantation into right coronary artery lesions by multimodality intracoronary imaging. *EuroIntervention*. 2016;12:1481-9.
- Oemrawsingh RM, Cheng JM, Garcia-Garcia HM, van Geuns RJ, de Boer SP, Simsek C, Kardys I, Lenzen MJ, van Domburg RT, Regar E, Serruys PW, Akkerhuis KM, Boersma E, ATHEROREMO-NIRS Investigators. Near-infrared spectroscopy predicts cardiovascular outcome in patients with coronary artery disease. *J Am Coll Cardiol*. 2014;64:2510-8.
- Schuurman AS, Vroegindewey M, Kardys I, Oemrawsingh RM, Cheng JM, de Boer S, Garcia-Garcia HM, van Geuns RJ, Regar ES, Daemen J, van Mieghem NM, Serruys PW, Boersma E, Akkerhuis KM. Near-infrared spectroscopy-derived lipid core burden index predicts adverse cardiovascular outcome in patients with coronary artery disease during long-term follow-up. *Eur Heart J*. 2018;39:295-302.
- Goldstein JA, Maini B, Dixon SR, Brilakis ES, Grines CL, Rizik DG, Powers ER, Steinberg DH, Shunk KA, Weisz G, Moreno PR, Kini A, Sharma SK, Hendricks MJ, Sum ST, Madden SP, Muller JE, Stone GW, Kern MJ. Detection of lipid core plaques by intracoronary near-infrared spectroscopy identifies high risk of periprocedural myocardial infarction. *Circ Cardiovasc Interv*. 2011;4:429-37.
- Stone GW, Maehara A, Muller JE, Rizik DG, Shunk KA, Ben-Yehuda O, Genereux P, Dressler O, Parvataneni R, Madden S, Shah P, Brilakis ES, Kini AS; CANARY Investigators. Plaque Characterization to Inform the Prediction and Prevention of Periprocedural Myocardial Infarction During Percutaneous Coronary Intervention: The CANARY Trial (Coronary Assessment by Near-infrared of Atherosclerotic Rupture-prone Yellow). *JACC Cardiovasc Interv*. 2015;8:927-36.
- Kini AS, Motoyama S, Vengrenyuk Y, Feig JE, Pena J, Baber U, Bhat AM, Moreno P, Kovacic JC, Narula J, Sharma SK. Multimodality Intravascular Imaging to Predict Periprocedural Myocardial Infarction During Percutaneous Coronary Intervention. *JACC Cardiovasc Interv*. 2015;8:937-45.
- Madder RD, Smith JL, Dixon SR, Goldstein JA. Composition of target lesions by near-infrared spectroscopy in patients with acute coronary syndrome versus stable angina. *Circ Cardiovasc Interv*. 2012;5:55-61.

12. Madder RD, Goldstein JA, Madden SP, Puri R, Wolski K, Hendricks M, Sum ST, Kini A, Sharma S, Rizik D, Brilakis ES, Shunk KA, Petersen J, Weisz G, Virmani R, Nicholls SJ, Maehara A, Mintz GS, Stone GW, Muller JE. Detection by near-infrared spectroscopy of large lipid core plaques at culprit sites in patients with acute ST-segment elevation myocardial infarction. *JACC Cardiovasc Interv*. 2013;6:838-46.
13. Garcia BA, Wood F, Cipher D, Banerjee S, Brilakis ES. Reproducibility of near-infrared spectroscopy for the detection of lipid core coronary plaques and observed changes after coronary stent implantation. *Catheter Cardiovasc Interv*. 2010;76:359-65.
14. Maini A, Buyantseva L, Maini B. In vivo lipid core plaque modification with percutaneous coronary revascularization: a near-infrared spectroscopy study. *J Invasive Cardiol*. 2013;25:293-5.
15. Noori M, Thayssen P, Veien KT, Junker A, Hansen KN, Hansen HS, Jensen LO. Lipid-core burden response to stent implantation assessed with near-infrared spectroscopy and intravascular ultrasound evaluation in patients with myocardial infarction. *Cardiovasc Revasc Med*. 2017;18:182-9.
16. Štěchovský C, Hájek P, Horváth M, Špaček M, Veselka J. Near-infrared spectroscopy combined with intravascular ultrasound in carotid arteries. *Int J Cardiovasc Imaging*. 2016;32:181-8.
17. Štěchovský C, Hájek P, Horváth M, Špaček M, Veselka J. Composition of carotid artery stenosis and restenosis: A series of patients assessed with intravascular ultrasound and near-infrared spectroscopy. *Int J Cardiol*. 2016;207:64-6.
18. North American Symptomatic Carotid Endarterectomy Trial Collaborators, Barnett HJM, Taylor DW, Haynes RB, Sackett DL, Peerless SJ, Ferguson GG, Fox AJ, Rankin RN, Hachinski VC, Wiebers DO, Eliasziw M. Beneficial effect of carotid endarterectomy in symptomatic patients with high-grade carotid stenosis. *N Engl J Med*. 1991;325:445-53.
19. European Stroke Organisation, Tendera M, Aboyans V, Bartelink ML, Baumgartner I, Clément D, Collet JP, Cremonesi A, De Carlo M, Erbel R, Fowkes FG, Heras M, Kownator S, Minar E, Ostergren J, Poldermans D, Rimbau V, Roffi M, Röther J, Sievert H, van Sambeek M, Zeller T; ESC Committee for Practice Guidelines. ESC Guidelines on the diagnosis and treatment of peripheral artery diseases: Document covering atherosclerotic disease of extracranial carotid and vertebral, mesenteric, renal, upper and lower extremity arteries: the Task Force on the Diagnosis and Treatment of Peripheral Artery Diseases of the European Society of Cardiology (ESC). *Eur Heart J*. 2011;32:2851-906.
20. Veselka J, Cerná D, Zimolová P, Blasko P, Fiedler J, Hájek P, Malý M, Zemánek D, Duchonová R. Thirty-day outcomes of direct carotid artery stenting with cerebral protection in high-risk patients. *Circ J*. 2007;71:1468-72.
21. Spacek M, Martinkovicova L, Zimolova P, Veselka J. Mid-term outcomes of carotid artery stenting in patients with angiographic string sign. *Catheter Cardiovasc Interv*. 2012;79:174-9.
22. Mintz GS, Nissen SE, Anderson WD, Bailey SR, Erbel R, Fitzgerald PJ, Pinto FJ, Rosenfield K, Siegel RJ, Tuzcu EM, Yock PG. American College of Cardiology Clinical Expert Consensus Document on Standards for Acquisition, Measurement and Reporting of Intravascular Ultrasound Studies (IVUS). A report of the American College of Cardiology Task Force on Clinical Expert Consensus Documents. *J Am Coll Cardiol*. 2001;37:1478-92.
23. Rosenfield K, Matsumura JS, Chaturvedi S, Riles T, Ansel GM, Metzger DC, Wechsler L, Jaff MR, Gray W; ACT I Investigators. Randomized Trial of Stent versus Surgery for Asymptomatic Carotid Stenosis. *N Engl J Med*. 2016;374:1011-20.
24. Brott TG, Howard G, Roubin GS, Meschia JF, Mackey A, Brooks W, Moore WS, Hill MD, Mantese VA, Clark WM, Timaran CH, Heck D, Leimgruber PP, Sheffet AJ, Howard VJ, Chaturvedi S, Lal BK, Voeks JH, Hobson RW 2nd; CREST Investigators. Long-Term Results of Stenting versus Endarterectomy for Carotid-Artery Stenosis. *N Engl J Med*. 2016;374:1021-31.
25. Reimers B, Nikas D, Stabile E, Favero L, Saccà S, Cremonesi A, Rubino P. Preliminary experience with optical coherence tomography imaging to evaluate carotid artery stents: safety, feasibility and techniques. *EuroIntervention*. 2011;7:98-105.
26. Jones MR, Attizzani GF, Given CA 2nd, Brooks WH, Ganocy SJ, Ramsey CN, Fujino Y, Bezerra HG, Costa MA. Intravascular frequency-domain optical coherence tomography assessment of carotid artery disease in symptomatic and asymptomatic patients. *JACC Cardiovasc Interv*. 2014;7:674-84.

Supplementary data

Supplementary Appendix 1. Intravascular ultrasound analysis and definitions.

Supplementary Table 1. Stents and protection devices utilised in the study.

Supplementary Table 2. Baseline LCBI in subgroups of patients.

Supplementary Table 3. Lipid signal after CAS with open- vs. closed- or hybrid-cell stents.

The supplementary data are published online at:

<https://eurointervention.pconline.com/>

doi/10.4244/EIJ-D-17-01054



Supplementary data

Supplementary Appendix 1. Intravascular ultrasound analysis and definitions

The definitions of the IVUS measurements used in the study are identical to those reported in the expert consensus document²². Semi-automated contour detection with manual corrections of the luminal border and the external elastic membrane (EEM) were performed. Lumen cross-sectional area (CSA) is the area bounded by the luminal border. MLA is the lumen CSA with the minimal area. EEM CSA (or vessel area) is the area bounded by the EEM border. PB is the EEM CSA minus the lumen CSA, divided by the EEM CSA. PB represents vessel area occupied by the atheroma regardless of lumen compromise. The extent of calcifications was measured in degrees (arc of calcium) at the cross-sectional IVUS image at the site of MLA. The cross-sectional frame used as the distal reference was the most distal IVUS frame with detectable lumen and EEM. Plaques at the site of MLA were defined as fibrocalcific if any calcifications were present and fibrous if there were no calcifications.

Supplementary Table 1. Stents and protection devices utilised in the study.

	N (%)
Distal filter	113 (94%)
Emboshield NAV6™ (Abbott Vascular, Santa Clara, CA, USA)	68 (57%)
FilterWire EZ™ (Boston Scientific, Marlborough, MA, USA)	45 (37%)
Proximal protection device	16 (13%)
Mo.Ma™ (Invatec, Roncadelle, Italy)	16 (13%)
Combination of both devices	9 (8%)
Stent	129
Xact™ (Abbott Vascular)	47 (36%)
sinus-Carotid™ (Optimed, Ettlingen, Germany)	33 (26%)
WALLSTENT™ (Boston Scientific)	36 (28%)
Cristallo Ideale™ (Invatec)	13 (10%)

Supplementary Table 2. Baseline LCBI in subgroups of patients.

	n (%)	LCBI, median (IQR)	<i>p</i> -value	LCBI _{max} , median (IQR)	<i>p</i> -value	LCBI _{mla} , median (IQR)	<i>p</i> -value
Sex							
Male	75 (67%)	75 (30-152)	0.096	315 (173-467)	0.213	177 (0-347)	0.196
Female	37 (33%)	56 (21-84)		289 (151-362)		76 (0-241)	
Symptomatic stenosis							
Yes	17 (14%)	88 (56-179)	0.098	381 (271-543)	0.100	300 (0-495)	0.587
No	103 (86%)	57 (25-104)		291 (157-428)		122 (1-286)	
Coronary artery disease							
Yes	60 (50%)	56 (28-153)	0.825	293 (155-480)	0.938	120 (0-298)	0.949
No	60 (50%)	67 (31-102)		296 (203-426)		172 (0-338)	
Statin therapy at baseline							
Yes	92 (77%)	65 (29-126)	0.511	294 (174-449)	0.873	159 (0-337)	0.396
No	28 (23%)	67 (47-153)		314 (244-422)		41 (0-267)	

LCBI: lipid core burden index; LCBI_{max}: maximal lipid core burden index in any 4 mm segment of the artery;

LCBI_{mla}: lipid core burden index in the 4 mm segment at the site of minimal luminal area

Supplementary Table 3. Lipid signal after CAS with open- vs. closed- or hybrid-cell stents.

	Open-cell stents	Closed- and hybrid-cell stents	<i>p</i> -value
Baseline LCBI	77 (25-176)	57 (26-105)	0.304
Post-stent LCBI	11 (1-71)	7 (1-30)	0.258
Post-dilatation LCBI	9 (1-52)	4 (0-34)	0.170

CAS: carotid artery stenting; LCBI: lipid core burden index